

Polarization-independent Pancharatnam-Berry phase lens system

TAO ZHAN, JIANGHAO XIONG, YUN-HAN LEE, AND SHIN-TSON WU*

CREOL, The College of Optics and Photonics, University of Central Florida, Orlando, FL 32816, USA
*swu@creol.ucf.edu

Abstract: The conventional liquid crystal-based Pancharatnam-Berry (PB) phase lens exhibits distinct polarization selectivity, manifesting opposite optical power to circularly polarized light with opposite handedness. Here, a polarization-independent liquid crystal PB lens system is theoretically predicted and experimentally verified. Such a lens system consists of at least four PB lenses, with specific distances in between them. This enables the PB lens to be applied in polarization-independent optical systems.

© 2018 Optical Society of America under the terms of the [OSA Open Access Publishing Agreement](#)

1. Introduction

The significant limitations of conventional refractive optical elements, including but not limited to bulkiness, heaviness and high fabrication cost, have never been addressed so apparently as in recent years, due to the emerging development and commercialization of portable and wearable devices. Instead, functional planar optical elements [1–4] based on Pancharatnam-Berry (PB) phase are gaining popularity, especially those made of liquid crystals (LCs), for their nearly 100% diffraction efficiency, excellent optical quality, and low cost. The phase of planar PB optical elements can be precisely controlled by spatial-varying LC anisotropy, including gratings [5,6], lenses [7–10], axicons [2] and general holograms, thus could be well utilized not only for scientific research but also for field applications [11–17]. However, since LC based PB optical element is intrinsically polarization-dependent, that is to say, if a PB lens converges the incident right-handed circularly polarized (RCP) light, then it will diverge the LCP light. As a result, polarization control is usually necessary in order to function like a traditional polarization-independent optical element for imaging.

In the paper, we demonstrate the feasibility to design a polarization-independent Pancharatnam-Berry phase lens (PBL) system manifesting same optical function for all polarizations. This is made possible by combining several PBLs together with specific distances in between. Firstly, ray transfer matrix analysis is utilized to derive the required constraints for polarization independency. Then, four PBLs with desired optical power are fabricated and assembled together in the pre-designed manner as a polarization-independent PBL system.

2. Design

A PBL is essentially a LC wave-plate with parabolic patterned anisotropy axis orientation, as depicted in Figs. 1(a) and 1(b). Considering RCP and LCP manifest opposite PB phase for the same LC pattern [11], PBL has opposite optical power for the incident light with opposite handedness as shown in Fig. 1(c). The multi-PBL system, as shown in Fig. 1(d), is designed principally with ray tracing method in matrix formulation for simplicity. Typically, the thickness of a PBL is only few microns, so it is reasonable to apply the thin lens approximation in matrix form:

$$K = \begin{pmatrix} 1 & 0 \\ (-1) \frac{s_3+1}{2} k & 1 \end{pmatrix}, \quad (1)$$

where k is the optical power (in diopter) of the PBL for RCP light and S_3 is the 4th Stokes parameter, which defines the handedness of polarization. It is worth mentioning that handedness switches every time when the light passes through a PBL. For a lens system made of PBLs, the system ray transfer matrix could be written as:

$$M_{i,S_3} = \begin{pmatrix} A_{i,S_3} & B_{i,S_3} \\ C_{i,S_3} & D_{i,S_3} \end{pmatrix} = K_1 D_1 K_2 D_2 \cdots K_{i-1} D_{i-1} K_i, \quad (2)$$

where K_i is the i^{th} PBL ray transfer matrix for the RCP light incident on the system, D_i is the propagation ray transfer matrix for the distance between i^{th} and $(i + 1)^{\text{th}}$ PBL:

$$K_i = \begin{pmatrix} 1 & 0 \\ (-1)^{i+\frac{S_3-1}{2}} k_i & 1 \end{pmatrix}, \quad (3)$$

and

$$D_i = \begin{pmatrix} 1 & d_i \\ 0 & 1 \end{pmatrix}. \quad (4)$$

In Eq. (3), k_i is the optical power of the i^{th} PBL for RCP light, and in Eq. (4), d_i is the effective optical distance between the i^{th} and $(i + 1)^{\text{th}}$ PBL.

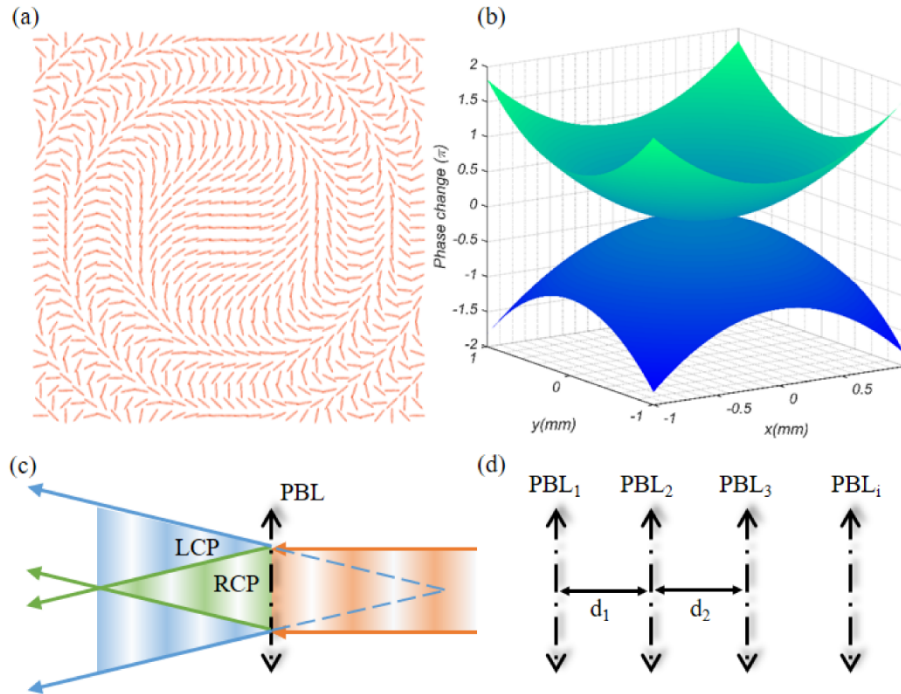


Fig. 1. (a) Top view of the distribution of LC anisotropy axis orientation. (b) phase profile of a PBL with opposite optical power for RCP and LCP, respectively (c) PBL functions as a diverging lens for LCP light but a converging lens for RCP light (d) Notation of PBL system.

2.1 Two-PBL system

For an optical system with two PBLs, the system ray transfer matrix can be derived as:

$$M_{2,S_3} = \begin{pmatrix} A_{2,S_3} & B_{2,S_3} \\ C_{2,S_3} & D_{2,S_3} \end{pmatrix} = \begin{pmatrix} 1 + (-1)^{\frac{S_3+3}{2}} k_2 d_1 & d_1 \\ (-1)^{\frac{S_3+1}{2}} k_1 + (-1)^{\frac{S_3+3}{2}} k_2 - k_1 k_2 d_1 & 1 + (-1)^{\frac{S_3+1}{2}} k_1 d_1 \end{pmatrix}. \quad (5)$$

In order to be polarization-independent, there must be:

$$M_{2,+1} = M_{2,-1}. \quad (6)$$

Equivalently,

$$\begin{cases} 1 + k_2 d_1 = 1 - k_2 d_1 \\ d_1 = d_1 \\ -k_1 + k_2 - k_1 k_2 d_1 = k_1 - k_2 - k_1 k_2 d_1 \\ 1 - k_1 d_1 = 1 + k_1 d_1 \end{cases} \quad (7)$$

Apparently, there is no nontrivial solution for the 2-PBL system to be polarization-independent. Although a 2-PBL system cannot show polarization-independent imaging, it could focus a collimated RCP and LCP light into the same spot [7], manifesting polarization-independent back focal length, whose requirement could be shown in our matrix formulation as:

$$BFL = -\frac{A_{2,+1}}{C_{2,+1}} = -\frac{A_{2,-1}}{C_{2,-1}}, \quad (8)$$

which could be satisfied with:

$$d_1 = \sqrt{\frac{1}{k_2^2} - \frac{1}{k_1 k_2}}. \quad (9)$$

2.2 Three-PBL system

Similarly, for a polarization-independent optical system with three PBLs, there must be:

$$M_{3,+1} = M_{3,-1}. \quad (10)$$

Equivalently,

$$\begin{cases} d_1 k_2 - d_1 k_3 - d_2 k_3 = 0 \\ d_1 d_2 k_2 = 0 \\ k_2 - k_1 - k_3 + d_1 d_2 k_1 k_2 k_3 = 0 \\ d_2 k_2 - d_2 k_1 - d_1 k_1 = 0 \end{cases} \quad (11)$$

Considering the existence of the second sub-equation in Eq. (11), no matter what the solutions are, the 3-PBL system turns out to be a 2-PBL system. As a result, the whole system cannot be a 3-PBL system and it is still impossible to achieve polarization independent imaging.

2.3 Four-PBL system

Eventually, the polarization independence could be enabled by a 4-PBL system, where enough degree of freedom and symmetry are available. By solving:

$$M_{4,+1} = M_{4,-1}, \quad (12)$$

we find:

$$\begin{cases} d_1k_2 - d_1k_3 + d_1k_4 - d_2k_3 + d_2k_4 + d_3k_4 - d_1d_2d_3k_2k_3k_4 = 0 \\ d_1d_2k_2 + d_1d_3k_2 - d_1d_3k_3 - d_2d_3k_3 = 0 \\ k_2 - k_1 - k_3 + k_4 + d_1d_2k_1k_2k_3 - d_1d_2k_1k_2k_4 - d_1d_3k_1k_2k_4 + d_1d_3k_1k_3k_4 \\ + d_2d_3k_1k_3k_4 - d_2d_3k_2k_3k_4 = 0 \\ d_2k_2 - d_2k_1 - d_1k_1 - d_3k_1 + d_3k_2 - d_3k_3 + d_1d_2d_3k_1k_2k_3 = 0 \end{cases} \quad (13)$$

There are two sets of nontrivial solutions to Eq. (13) as shown in Eq. (14). With appropriate arrangement the optical power of each lens can be derived as a function of distances between each two of them.

$$\begin{cases} k_1 = \frac{d_3(d_2 + d_3)}{d_1(d_1 + d_2)} \\ k_2 = \pm \frac{(d_1d_3 + d_2d_3)}{2d_3^2(d_1d_2 + d_2d_3)} \times \\ \left(\sqrt{4d_3^2d_3^2 + d_2^2 + 8d_2d_3^2 + 4d_1d_2d_3^2 + d_1d_2 + 4d_3^4 + 4d_1d_3^3} \pm 1 \right) \\ k_3 = \pm \frac{1}{2d_3^2} \left(\frac{\sqrt{4d_2^2d_3^2 + d_2^2 + 8d_2d_3^2 + 4d_1d_2d_3^2 + d_1d_2 + 4d_3^4 + 4d_1d_3^3} \pm 1}{d_2(d_1 + d_2)} \right) \\ k_4 = 1 \end{cases} \quad (14)$$

For the simplest cases $d_1 = d_2 = d_3 = d$, we can find following simple solutions:

$$\begin{cases} k_1 = k_4 = 1 \\ k_2 = k_3 = \pm \frac{\sqrt{1+12d^2} \pm 1}{2d^2} \end{cases} \quad (15)$$

For the symmetric cases $d_1 = d_3$, the solution can be derived as:

$$\begin{cases} k_1 = k_4 = 1 \\ k_2 = k_3 = \pm \frac{\sqrt{1+4d_1^2 + 8d_1^3/d_2} \pm 1}{2d_1^2} \end{cases} \quad (16)$$

The total optical power of the 4-PBL system (in the simplest cases mentioned in Eq. (15)) is evaluated for both sets of solutions. Results are plotted in Figs. 2(a) and 2(b). The (+/-) solution shows a relatively small optical power (0~1.1D), as compared to the (+/-) solution. The system optical power in the symmetric case mentioned in Eq. (16) is also evaluated for both sets of solutions, and results are plotted in Figs. 2(c) and 2(d). Similarly, the optical power of the (+/-) solution (0~3.6D) is smaller than that of the (+/-) solution.

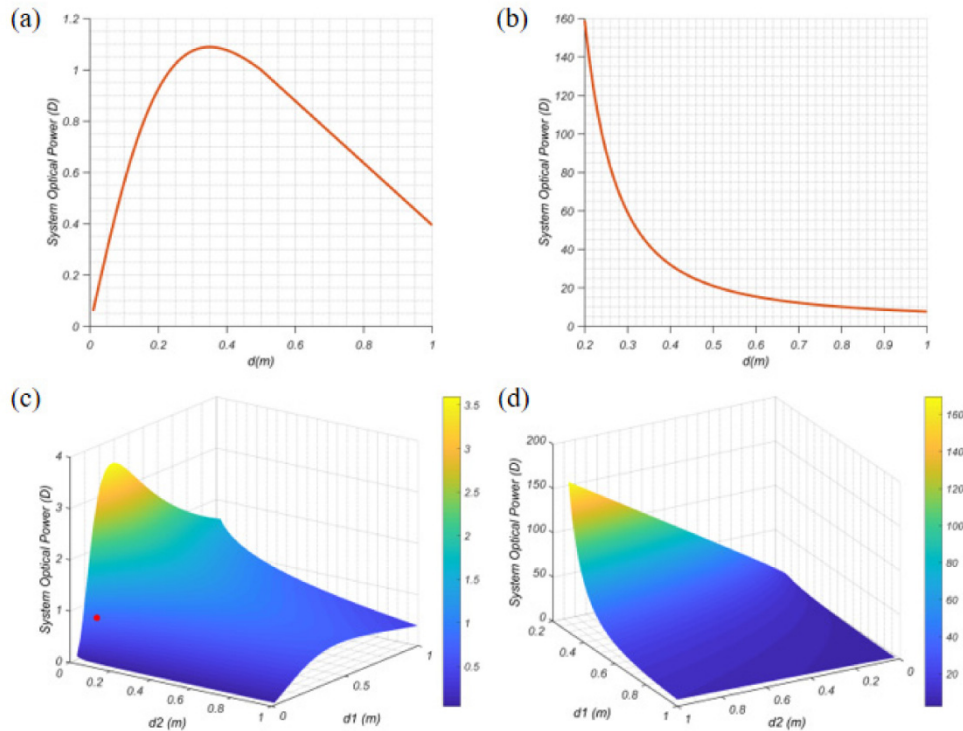


Fig. 2. Simulated system optical power for the solutions of Eq. (15): (a) for (+, -), (b) for (-, +), and Eq. (16): (c) for (+, -), (d) for (-, +).

3. Experiment

3.1 Device fabrication

To prove concept, we fabricated four PBLs according to a symmetric solution with $k_1 = k_4 = 1$ diopter and $k_2 = k_3 = 10$ diopters, as marked by the red dot in Fig. 2(c). We then assembled the 4 PBLs into a symmetric system, with $d_1 = d_3 = 46.1$ mm, and $d_2 = 10.0$ mm. The calculated system effective focal length is around 1.1 m and back focal length is around 1 m. Photo-alignment method was applied to fabricate the PBLs [14]. A thin photo-alignment material (Brilliant Yellow, from Sigma-Aldrich, dissolved in dimethyl-formamide with 0.2wt% concentration) was spin-coated on a glass substrate with 500rpm for 5s and 3000rpm for 30s. The coated substrate was directly exposed by a desired interference pattern generated by the optical setup shown in Fig. 3. A collimated linearly polarized laser beam ($\lambda = 457$ nm) was split into two arms after passing through a non-polarizing beam splitter (BS). One beam was converted to LCP by a quarter-wave plate functioning as the reference beam, while the other beam was converted to RCP. These two laser beams were supposed to have the same intensity on the prepared substrate (S), which was coated with a thin photo-alignment film, after being combined together by the 2nd beam splitter. The optical power and active area of fabricated lens could be easily tuned by the positions of the two refractive lenses, L_1 and L_2 . This polarization holography setup enables the fabrication of large size PBLs with high quality. The PBLs was exposed to the laser beam with intensity ~ 0.3 mW/cm² for 4 min.

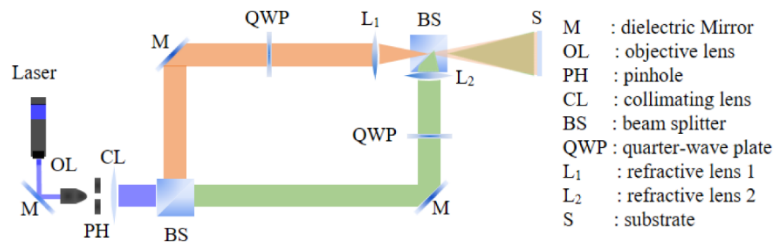


Fig. 3. The optical setup of exposure procedure in the PBL fabrication process.

After exposure, the substrate was coated with a liquid crystal solution which contains 20 wt.% LC monomer RM257 and 0.6 wt.% photo-initiator Irgacure 651, balanced in Toluene. The thickness of RM257 film is controlled by spin-coating speed (500rpm for 5s then 3000rpm for 30s) to satisfy the half-wave requirement ($d\Delta n = \lambda/2$) for green light, and then the samples were cured by UV light (365nm) in N_2 -rich environment, forming a cross-linked LC polymeric lens. The optical axis of the four fabricated PB lenses are aligned with the collimated laser beam, satisfying the paraxial approximation of the design.

3.2 Experimental verification

The polarization independence of fabricated 4-PBL system is tested by two means. Firstly, as shown in Fig. 4(a), a collimated laser beam (532nm, where PBLs' diffraction efficiency > 95%) is incident on both single PBL and 4-PBL system to test the focusing efficiency for different polarization states. A polarizer and a quarter-wave plate are utilized to change the polarization state of incident light. A single PBL works as a focusing lens only for one handedness, while the proposed 4-PBL system works for both, as indicated in Fig. 4(b), where the measured intensity was normalized to the maximum value for each case. It should also be mentioned that the absolute intensity for the 4-PBL system is around 82% of that of a single PBL, due to multiple interface reflections (without anti-reflection coating) and diffraction efficiency loss. Also, the 4-PBL can image object with unpolarized light to a single depth, while a single PBL always shows two imaging depths for the RCP and LCP lights, as shown in Fig. 4(c). The target in the images is a white paper with 'UCF' characters under green LED illumination, which is placed around 30 cm behind the 4-PBL system.

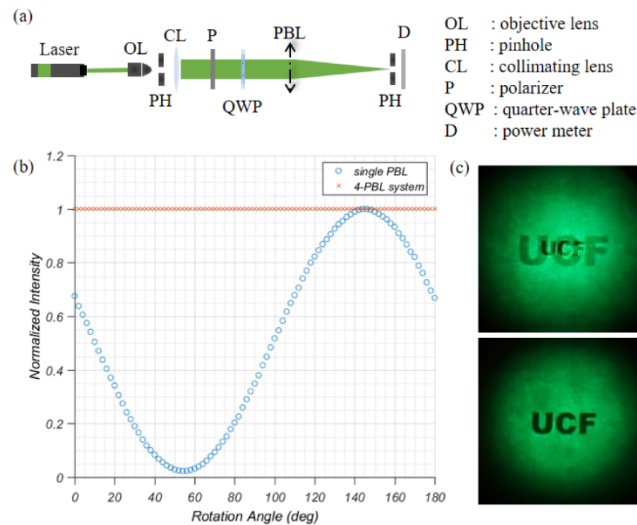


Fig. 4. (a) The optical setup to test PBL's polarization dependency. (b) Normalized intensity versus the relative angle between polarizer and fast-axis of quarter-wave plate. (c) Photos taken through a single PBL (upper) and a polarization independent 4-PBL system (lower).

4. Discussion

Compared to conventional refractive lenses, the polarization-independent PBL system has opposite chromatic dispersion, which could be utilized to reduce the chromatic aberrations in conventional refractive lens systems. It is also worthwhile to mention that there are 3-layer structure designs for single PBL with reduced color dispersion [18] and dual-twist [5] structure to increase the diffraction efficiency of single PBLs in the whole visible spectrum. Considering the correlation between the optical power of single PBLs and the distance between them, the degree of freedom in the proposed system is not as many as that in a conventional refractive system. In our formulation, maintaining the same back focal length for both RCP and LCP only needs the A/C value in the system ABCD matrix to be the same for the two polarizations. Thus, a system with two [7] or three [19] PBLs is sufficient to provide the necessitated degree of freedom. Moreover, if all the four employed PBLs are active-driving [14], then the whole system could switch its optical power to zero by simply applying the same voltage to the 4 PBLs simultaneously. Also, if more than four PBLs are employed, then the optical power of the whole system could switch between its original one to another non-zero value without losing polarization independency. For example, in an active-driving 6-PBL system where only 4 of them have optical power (i.e. no voltage applied), then the system's optical power can be easily switched by choosing different set of 4 PBLs.

5. Conclusion

The possibility of a polarization-independent Pancharatnam-Berry phase lens system is theoretically predicted and experimentally demonstrated. The 4-PBL system, utilizing the compensation of different polarization dependency of each PBL, is able to provide single-depth high-resolution images for viewers without preprocessing the incident polarization state. Considering its low cost and simple fabrication process, the proposed PBL system has potential to replace or to be integrated with refractive lenses for various optical applications.

Funding

Intel Corporation.

Acknowledgments

The authors would like to thank Zheyuan Zhu for valuable assistance in the experiment.

References

1. N. Yu and F. Capasso, "Flat optics with designer metasurfaces," *Nat. Mater.* **13**(2), 139–150 (2014).
2. J. Kim, Y. Li, M. N. Miskiewicz, C. Oh, M. W. Kudenov, and M. J. Escuti, "Fabrication of ideal geometric phase holograms with arbitrary wavefronts," *Optica* **2**(11), 958–964 (2015).
3. N. V. Tabiryan, S. R. Nersisyan, D. M. Steeves, and B. R. Kimball, "The promise of diffractive waveplates," *Opt. Photonics News* **21**(3), 41–45 (2010).
4. L. De Sio, D. E. Roberts, Z. Liao, S. Nersisyan, O. Uskova, L. Wickboldt, N. Tabiryan, D. M. Steeves, and B. R. Kimball, "Digital polarization holography advancing geometrical phase optics," *Opt. Express* **24**(16), 18297–18306 (2016).
5. C. Oh and M. J. Escuti, "Achromatic diffraction from polarization gratings with high efficiency," *Opt. Lett.* **33**(20), 2287–2289 (2008).
6. S. R. Nersisyan, N. V. Tabiryan, D. M. Steeves, and B. R. Kimball, "Optical axis gratings in liquid crystals and their use for polarization insensitive optical switching," *J. Nonlinear Opt. Phys. Mater.* **18**(01), 1–47 (2009).
7. N. V. Tabiryan, S. V. Serak, D. E. Roberts, D. M. Steeves, and B. R. Kimball, "Thin waveplate lenses of switchable focal length--new generation in optics," *Opt. Express* **23**(20), 25783–25794 (2015).
8. N. V. Tabiryan, S. V. Serak, S. R. Nersisyan, D. E. Roberts, B. Ya. Zeldovich, D. M. Steeves, and B. R. Kimball, "Broadband waveplate lenses," *Opt. Express* **24**(7), 7091–7102 (2016).
9. Z. He, Y. H. Lee, R. Chen, D. Chanda, and S. T. Wu, "Switchable Pancharatnam-Berry microlens array with nano-imprinted liquid crystal alignment," *Opt. Lett.* **43**(20), 5062–5065 (2018).
10. K. Gao, H. H. Cheng, A. Bhowmik, C. McGinty, and P. Bos, "Nonmechanical zoom lens based on the Pancharatnam phase effect," *Appl. Opt.* **55**(5), 1145–1150 (2016).
11. Y. H. Lee, G. Tan, T. Zhan, Y. Weng, G. Liu, F. Gou, F. Peng, N. V. Tabiryan, S. Gauza, and S. T. Wu, "Recent progress in Pancharatnam-Berry phase optical elements and the applications for virtual/augmented realities," *Opt. Data Process. Storage* **3**(1), 79–88 (2017).
12. X. Xiang, J. Kim, R. Komanduri, and M. J. Escuti, "Nanoscale liquid crystal polymer Bragg polarization gratings," *Opt. Express* **25**(16), 19298–19308 (2017).
13. Y. H. Lee, T. Zhan, and S. T. Wu, "Enhancing the resolution of a near-eye display with a Pancharatnam-Berry phase deflector," *Opt. Lett.* **42**(22), 4732–4735 (2017).
14. T. Zhan, Y. H. Lee, and S. T. Wu, "High-resolution additive light field near-eye display by switchable Pancharatnam-Berry phase lenses," *Opt. Express* **26**(4), 4863–4872 (2018).
15. G. Tan, Y. H. Lee, T. Zhan, J. Yang, S. Liu, D. Zhao, and S. T. Wu, "Foveated imaging for near-eye displays," *Opt. Express* **26**(19), 25076–25085 (2018).
16. F. Gou, F. Peng, Q. Ru, Y. H. Lee, H. Chen, Z. He, T. Zhan, K. L. Vodopyanov, and S. T. Wu, "Mid-wave infrared beam steering based on high-efficiency liquid crystal diffractive waveplates," *Opt. Express* **25**(19), 22404–22410 (2017).
17. Y. H. Lee, G. Tan, K. Yin, T. Zhan, and S. T. Wu, "Compact see-through near-eye display with depth adaption," *J. Soc. Inf. Disp.* **26**(2), 64–70 (2018).
18. D. Roberts, Z. Liao, J. Y. Hwang, S. R. Nersisyan, and N. Tabiryan, "Chromatic aberration corrected switchable optical systems," *Proc. SPIE* **10735**, 107350Q (2018).
19. N. V. Tabiryan, D. E. Roberts, D. M. Steeves, and B. R. Kimball, "Diffractive Waveplate Lenses for Correcting Aberrations and Polarization-Independent Functionality," U.S. Patent Application No. 14/688,256.